



**HAL**  
open science

# Telechelic polyethylene, poly(ethylene-co-vinyl acetate) and triblock copolymers based on ethylene and vinyl acetate by iodine transfer polymerization

Florian Baffie, Muriel Lansalot, Vincent Monteil, Franck d'Agosto

## ► To cite this version:

Florian Baffie, Muriel Lansalot, Vincent Monteil, Franck d'Agosto. Telechelic polyethylene, poly(ethylene-co-vinyl acetate) and triblock copolymers based on ethylene and vinyl acetate by iodine transfer polymerization. *Polymer Chemistry*, 2022, 13 (17), pp.2469-2476. 10.1039/D2PY00156J . hal-03722112

**HAL Id: hal-03722112**

**<https://hal.science/hal-03722112>**

Submitted on 13 Jul 2022

**HAL** is a multi-disciplinary open access archive for the deposit and dissemination of scientific research documents, whether they are published or not. The documents may come from teaching and research institutions in France or abroad, or from public or private research centers.

L'archive ouverte pluridisciplinaire **HAL**, est destinée au dépôt et à la diffusion de documents scientifiques de niveau recherche, publiés ou non, émanant des établissements d'enseignement et de recherche français ou étrangers, des laboratoires publics ou privés.



## Telechelic polyethylene, poly(ethylene-co-vinyl acetate) and triblock copolymers based on ethylene and vinyl acetate by iodine transfer polymerization.

Florian Baffie, Muriel Lansalot, Vincent Monteil,\* Franck D'Agosto\*

Received 00th January 20xx,  
Accepted 00th January 20xx

DOI: 10.1039/x0xx00000x

[www.rsc.org/](http://www.rsc.org/)

Various iodo functionalized chain transfer agents (CTAs) were successfully employed in the iodine transfer polymerization (ITP) of ethylene conducted at 80 bars at 70°C in dimethylcarbonate. Comparative studies performed on I-C<sub>6</sub>F<sub>12</sub>-I, C<sub>6</sub>F<sub>13</sub>-I, C<sub>6</sub>F<sub>12</sub>(CH<sub>2</sub>)<sub>2</sub>-I and C<sub>5</sub>H<sub>10</sub>-I mediated ITPs revealed that when I-C<sub>6</sub>F<sub>12</sub>-I was used as CTA the very first ethylene additions resulted in the formation of diiodo oligomeric compounds with various chain transfer activities. This however did not impede a good control of the polymerization that was rapidly installed. This allows the formation of well-defined telechelic polyethylene (I-PE-I) and poly(ethylene-co-vinyl acetate) (I-EVA-I) by ITP. I-EVA-I telechelic copolymers were further used as macromolecular CTAs in chain extension experiments in the presence of ethylene to lead to PE-*b*-EVA-*b*-PE triblock copolymers with different content of VAc (27 and 64 mol%) in the central EVA block.

### Introduction

Polyethylene (PE) exhibits excellent chemical resistance, mechanical properties and thermal stability. PE-based materials cover a wide range of applications ranging from commodity plastics (food packaging or trash bags) to high added value products (bulletproof vests or medical devices).<sup>1</sup> Given the industrial importance of PE, extensive research has naturally focused on the formation of functional PE including telechelics.<sup>2-7</sup> Telechelic polymers can have commercial applications as cross-linkers, building blocks or for further processing.<sup>8,9</sup> Telechelic PEs have been synthesized by different approaches, such as (i) pyrolysis<sup>10</sup> (ii) polymerization of butadiene followed by post-modification (hydrogenation, functionalization, ethenolysis),<sup>11-13</sup> (iii) ring-opening metathesis polymerization of cyclic olefins in the presence of a chain transfer agent followed by functionalization and hydrogenation,<sup>14-18</sup> (iv) living coordinative polymerization of ethylene followed by post-functionalization,<sup>19, 20, 21</sup> (v) selective coordination-insertion polymerization of ethylene in the presence of furan-derived monomers,<sup>22</sup> or (vi) catalyzed chain-growth polymerization of ethylene in the presence of functionalized chain transfer agent.<sup>23-27</sup> The last three strategies are based on the direct use of ethylene and are probably the most challenging ones.

Reversible-deactivation radical polymerization (RDRP)<sup>28</sup> implicitly provides polymer chains that are by essence telechelic since they carry the memory of the controlling agents used on both chain ends. Successful RDRPs of ethylene are thus by definition efficient tools to produce telechelic polyethylene directly from ethylene monomer and without additional chemical steps.

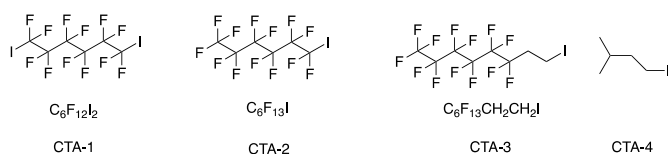
Despite its success for most vinylic monomers, the RDRP of some monomers of major industrial importance such as ethylene is still challenging. While the obtainment of well-defined copolymers with low ethylene incorporation have been reported,<sup>29, 30</sup> progresses over ethylene controlled radical polymerization have only been made over the last ten years using RDRPs based on degenerative chain transfer process. These include reversible addition-fragmentation chain transfer (RAFT),<sup>31-33</sup> organotellurium mediated radical polymerization (TERP)<sup>34</sup> or iodine transfer polymerization (ITP)<sup>35</sup> techniques. These systems are now able to control the polymerization of ethylene and its copolymerization with vinyl acetate (VAc) to produce well-defined poly(ethylene-co-vinyl acetate) (EVA). Very recently, the use of a trifunctional dithiocarbamate offered the possibility to synthesize an original three-arm EVA star copolymer.<sup>33</sup> Even if control of ethylene polymerization has not yet been achieved by Co-mediated radical polymerization (CMRP), triblock and macrocycles based on ethylene and VAc have nevertheless been synthesized.<sup>36-38</sup>

Concerning ITP, the use of chain transfer agents (CTAs) with two active iodine atoms such as I-C<sub>6</sub>F<sub>12</sub>-I (CTA-1) reported in **Scheme 1** has already been reported to prepare polymers bearing iodine at both polymer chain-ends by ITP.<sup>39 40-43</sup> CTA-1 is commercially available, cheap, rather insensitive to light. Its structure is

Univ Lyon, Université Claude Bernard Lyon 1, CPE Lyon, CNRS, UMR 5128, Catalysis, Polymerization, Processes and Materials (CP2M), 43 Bd du 11 Novembre 1918, 69616 Villeurbanne, France. [franck.dagosto@univ-lyon1.fr](mailto:franck.dagosto@univ-lyon1.fr), [vincent.monteil@univ-lyon1.fr](mailto:vincent.monteil@univ-lyon1.fr)

Electronic Supplementary Information (ESI) available: See DOI: 10.1039/x0xx00000x

indeed very similar to its monoiodo analogue  $C_6F_{13}I$  (CTA-2, **Scheme 1**) that we used to successfully control the ITP of ethylene and its copolymerization with VAc.<sup>35</sup> CTA-1 appeared thus as an ideal candidate to be tested for the synthesis of telechelic PEs. This is the purpose of the present paper, which investigates the synthesis via ITP of more complex macromolecular architectures, such as triblock copolymers, based on ethylene and vinyl acetate.



**Scheme 1.** Iodinated chain transfer agents (CTAs) used in this study.

## Experimental

### Materials

Ethylene (Air liquid, 99.95 %), 2,2'-azobis(isobutyronitrile) (AIBN, Aldrich, 98 %), dodecafluoro-1,6-diiodohexane (CTA-1, TCI, > 98 %), perfluorohexyl iodide (CTA-2, Aldrich, 99 %), 1H,1H,2H,2H-perfluorooctyl (CTA-3, Aldrich, 96 %) and 1-iodo-3-methylbutane (CTA-4, Aldrich, 97 %) were used as received. Dimethyl carbonate (DMC, Aldrich, 99 %) was used after bubbling with argon for more than 12 h. Vinyl acetate (VAc, Sigma, > 99 %) was purified over neutral alumina and was used after bubbling with argon for more than 12 h. Tetrachloroethylene (TCE, ACS reagent, Aldrich) was purified by passing through silica.

### Methods

**Homopolymerization of ethylene.** The employed stainless-steel reactor (160 mL, from Parr Instrument Co.) was equipped with a mechanical stirring apparatus, a thermometer, a pressure sensor and safety valves. For polymerization procedures, a solution of CTA and AIBN (50 mg, 0.30 mmol, 6.09 mmol L<sup>-1</sup>) in DMC (50 mL) was introduced through a cannula into an injecting chamber. The chamber was then pressurized at 20 bar of ethylene and opened into the preheated autoclave with a stirring speed of 600 rpm. Immediately after, ethylene gas was introduced into the reactor until a pressure of 80 or 200 bar was reached, which took about 4 min. To manage polymerization safely over 50 bar of ethylene, we used a 1.5 L intermediate tank. The tank was cool down to -20 °C to liquefy ethylene at 40 bar. When thermodynamic equilibrium was reached, the intermediate tank was isolated and heated to reach 80 or 200 bar. This tank was used to charge the reactor and to maintain a constant pressure of ethylene in the reactor by successive manual ethylene additions. After the desired time at 70 °C, the stirring was slowed down and the autoclave was cooled with iced water. When the temperature inside the autoclave dropped below 25 °C, the remaining pressure was carefully

released. The content of the reactor was collected with toluene. The evaporation of the solvent gave the polymer product.

**Copolymerization of ethylene and vinyl acetate.** In a typical polymerization procedure, a vinyl acetate, CTA and AIBN solution in DMC was prepared, such that the total volume was kept to 50 mL.

For the chain extension, the EVA macroCTA (0.45 mmol) and AIBN (25 mg, 0.15 mmol) were dissolved in the desired mixture of VAc/DMC (0/100 or 50/50 v/v) and degassed with argon for 30 min. The rest of the procedure remained the same as for ethylene homopolymerization except from the temperature and the solvent to recover the polymer which are here 80 °C and acetone.

### Characterization

**Nuclear magnetic resonance (NMR).** All NMR experiments were performed at 90 °C in 2:1 TCE/deuterated benzene ( $C_6D_6$ ) solutions or at 25 °C in deuterated chloroform ( $CDCl_3$ ) using a Bruker Avance 400 spectrometer (<sup>1</sup>H: 400.13 MHz; <sup>13</sup>C: 100.61 MHz). The temperature was calibrated with a tube containing 80 vol% of ethylene glycol and 20 vol% of DMSO-*d*<sub>6</sub>. Proton and fluor NMR spectra were recorded with a 5 mm BBFO+ probe with a z-gradient coil ( $D_1 = 3$  s, scans = 256, RO = 20 Hz with  $O_1P = 6.5$  and -78 ppm,  $O_2P = 4.5$  and 80 ppm for proton and fluor, respectively). Carbon NMR spectra were recorded with a 10 mm SEX probe, <sup>13</sup>C selective with a z-gradient coil. The pulse sequence used includes a decoupling proton with NOE effects, and a 70° spin excitation ( $D_1 = 2$  s, scans = 6144,  $O_1P = 110$  ppm,  $O_2P = 80$  ppm, RO = 20 Hz). The method is said to be "semiquantitative," and the NMR calculations were carried out between carbons of the same nature (the -CH<sub>2</sub>-). Chemical shifts are given in parts per million (ppm) with the solvent peak as internal standard.

**Size exclusion chromatography (SEC).** For THF insoluble polymer samples, molar mass measurements were performed using a Viscotek High-Temperature Triple Detection SEC (HT-SEC) system (Malvern Instruments) that incorporates a differential refractive index detector, a viscometer, and a light scattering detector. 1,2,4-trichlorobenzene (TCB) was used as the mobile phase at a flow rate of 1 mL min<sup>-1</sup>. TCB was stabilized with 2,6-di(tert-butyl)-4-methylphenol. The separation was carried out on three mixed bed columns (PLgel Olexis 300 × 7.8 mm from Malvern Instrument) and a guard column (75 × 7.5 mm). Columns and detectors were maintained at 150 °C. Sample volumes of 200 μL with concentration of 3 mg mL<sup>-1</sup> were injected and filtered online. The Omniseq software was used for data acquisition and data analysis. The number average molar mass ( $M_n$ ) and molar mass distribution (dispersity,  $\mathcal{D}$ ) was determined by means of a conventional calibration curve based on linear polyethylene standards from 300 to 130 000 g mol<sup>-1</sup> or by a universal calibration based on polystyrene (PS) standards (Polymer Standards Service).

For THF soluble polymer samples, molar mass measurements were performed using a Viscotek system (Malvern Instruments), including a four-capillary differential viscometer, a differential refractive index (RI) detector, and a UV detector. THF was used as the mobile phase at a flow rate of 1 mL min<sup>-1</sup>

at 35 °C. All samples were injected at a concentration of 3 to 6 mg mL<sup>-1</sup> after filtration through a 0.45 μm PTFE membrane. The separation was carried out on three Polymer Standard Service columns (SDVB, 5 μm, 300 × 7.5 mm) and a guard column.  $M_n$  and  $\mathcal{D}$  were determined by means of a conventional calibration curve based on polystyrene standards from 470 to 270 000 g mol<sup>-1</sup> or by a universal calibration based on PS standards (Polymer Standards Service). The Omniseq software was used for data acquisition and data analysis.

**Gas chromatography (GC)** analyses were conducted on a GC HP instrument 6890 equipped with a flame ionization detector (FID) and an Agilent 19091J-413 HP-5 column (30 m × 320 μm × 0.25 μm). Injector and detector temperatures were set to 250 °C. The initial and final column temperatures were respectively 40 °C and 250 °C, with a heating rate of 20 °C min<sup>-1</sup> and a final isotherm of 2 min at 250 °C. The internal standard used was dodecane.

**Differential scanning calorimetry (DSC)** DSC analyses were performed on a Mettler Toledo DSC 1. Measurements were carried by two successive heating and cooling cycles (10 °C min<sup>-1</sup>) with temperatures ranging from - 80 to + 150 °C. The melting and glass transition temperatures ( $T_m$  and  $T_g$ , respectively) were recorded on the second cycle.

## Results and discussion

**Telechelic PE. Kinetic investigations.** The experimental setup and conditions used to polymerize ethylene are similar to previous works from our group.<sup>31-35</sup> ITPs were conducted in a 160 mL autoclave reactor at 70 °C and at constant ethylene pressure (80 bar) in 50 mL of DMC. The ethylene consumption was determined gravimetrically after solvent evaporation. Our set up does not allow to withdraw aliquots during polymerization. Therefore, for the kinetics, each point represents a single experiment.

**Figure 1a** shows the ethylene consumption *versus* polymerization time for the ITP mediated by CTA-1, by C<sub>6</sub>F<sub>13</sub>-I (CTA-2) (**Scheme 1**) previously employed in our original works on ITP of ethylene,<sup>35</sup> and for a radical polymerization of ethylene conducted in absence of CTA. No rate retardation was observed with CTA-1 compared to the CTA-free system (nor with CTA-2, as already observed<sup>35</sup>). Moreover, as for CTA-2, CTA-1 was already totally converted after 45 minutes. For each system, the molar mass evolution *versus* ethylene consumption is presented in **Figure 1b**, and the corresponding molar mass distributions are given in **Figure 2**. The radical polymerization of ethylene yielded PE with  $M_n$  values around 8000 g mol<sup>-1</sup> and  $\mathcal{D}$  values between 1.5 and 2.1. As expected for ITP of ethylene, molar masses are relatively close to the theory. For the same iodine content ([CTA-2]:[AIBN] = 3:1 and [CTA-1]:[AIBN] = 1.5:1), they are two times higher for CTA-1 than for CTA-2 for the same ethylene consumption. This indicates that both iodines were reactivated to form telechelic PE chains. The evolution of  $M_n$  values (obtained by HT-SEC) with time follows the expected linear one, to reach up to 4100 g mol<sup>-1</sup> with dispersities around 1.5 (**Figure 1b**).

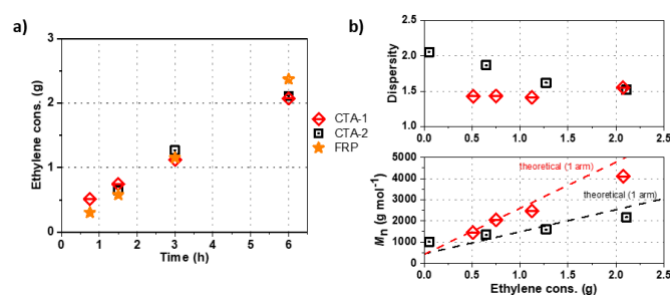


**Figure 1.** Ethylene consumption *versus* polymerization time for ITP systems compared to the conventional radical polymerization performed without CTA, and b) corresponding molar mass evolutions (from HT-SEC). Molar masses are determined by a conventional PE calibration. Polymerization conditions: T = 70 °C, P = 80 bar.

As already observed in our previous works, a low molar mass shoulder can be observed at short polymerization times for CTA-2 (**Figure 2b**). Mechanistically, this can be explained by faster chain deactivation in the pre-equilibrium than in the main equilibrium.<sup>35</sup> This phenomenon seems less pronounced for CTA-2 compared to CTA-1 (**Figure 2a**).

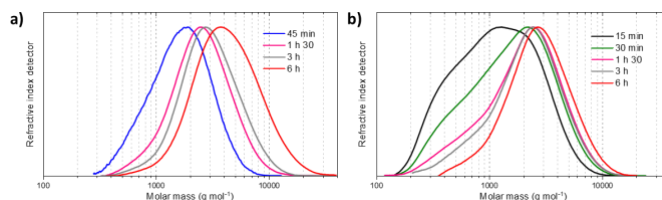


**Figure 2.** Molar mass distributions of PEs obtained during ITP of ethylene mediated by a) CTA-1 and b) CTA-2 at 70 °C and 80 bar of ethylene pressure after the indicated polymerization time (**Figure 1**). A conventional PE calibration was used.

The PE produced in presence of CTA-1 was analyzed by <sup>1</sup>H NMR for each polymerization time, with particular care taken to identify the polymer chain-ends. NMR spectra were recorded at 90 °C in the solvent mixture TCE/C<sub>6</sub>D<sub>6</sub> (2/1 v/v) (**Figure 3**). The iodine end-capped PE structure is proven by the signal of the methylene hydrogen atoms adjacent to the iodine atom (a, -CH<sub>2</sub>I at 2.95 ppm and b, -CH<sub>2</sub>CH<sub>2</sub>I at 1.65 ppm). As CTA-2, CTA-1 offers the possibility to see the methylene in α and β position to the -CF<sub>2</sub>- moiety (h, -C<sub>6</sub>F<sub>12</sub>CH<sub>2</sub>- at 1.90 ppm and g, -C<sub>6</sub>F<sub>12</sub>CH<sub>2</sub>CH<sub>2</sub>- at 1.50 ppm). A comparison of signal intensity of h and a indicates only a minimal loss of iodine chain-end functionality (< 5%) (**Figure 3d**). This illustrates the successful ITP of ethylene and the formation of the targeted telechelic PEs. It is nevertheless worth mentioning two other triplets of small intensity that can be observed at short polymerization times at 2.90 and 2.85 ppm (**Figure 3a**). Their intensities decrease over time (**Figure 3b-c**), and they disappear almost totally after 6 h of polymerization (**Figure 3d**). Such resonances were not present when using CTA-2.<sup>35</sup>

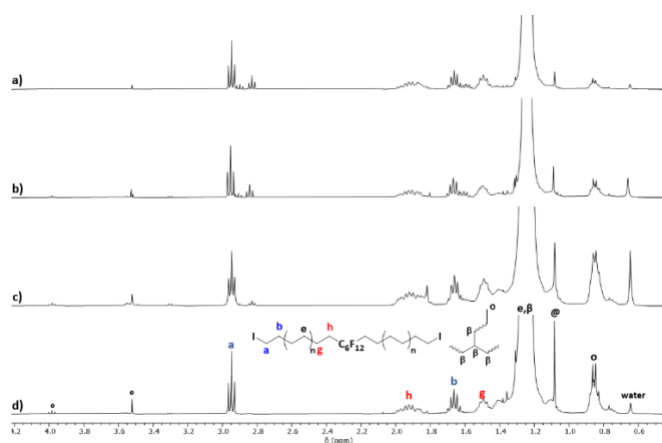


**Figure 3.**  $^1\text{H}$  NMR spectra (in  $\text{TCE}/\text{C}_6\text{D}_6$  at  $90^\circ\text{C}$ ) of PE synthesized at  $70^\circ\text{C}$ , 80 bar in the presence of CTA-1 after a) 45 min, b) 1 h 30, c) 3 h, and d) 6 h (see **Figure 1**). The end group  $-\text{CH}_3$  stems from intramolecular and intermolecular chain transfer inherent to ethylene radical polymerization. o: transfer to polymerization solvent DMC. @ stems from the isobutyronitrile chain-ends of the PE chains initiated by AIBN. The water is in the NMR solvent.

To elucidate the structure corresponding to the small resonances around 2.90 ppm in **Figure 3a**, 150 mg of the copolymer obtained after 45 min was purified by precipitation in methanol. The obtained solid was filtered and dried under vacuum to afford a white powder (135 mg). After evaporation of the filtrate, a white wax was obtained (15 mg). The solid and the residue from the filtrate were analyzed by  $^1\text{H}$  NMR (**Figure 4c and b**, respectively). The two triplets are almost no longer visible after precipitation. This observation, together with the recovering yield of the precipitation, confirmed that these resonances were corresponding to impurities and do not arise from a side reaction on the polymer backbone. Nevertheless, these two triplets are present in the spectrum of the filtrate residue with a multiplet that can clearly be seen at 1.60 ppm. This signal was indeed visible in the original polymer in **Figure 4a**. The average molar mass of the filtrate residue, determined from these  $^1\text{H}$  NMR analyses is around  $750\text{ g mol}^{-1}$ . The corresponding structure would then include approximately seven ethylene units added onto CTA-1. We thus assumed the formation of PE oligomers during the initial steps of the ITP, representing less than 10 wt% of the polymer produced after 45 min (15 mg over 150 mg purified).

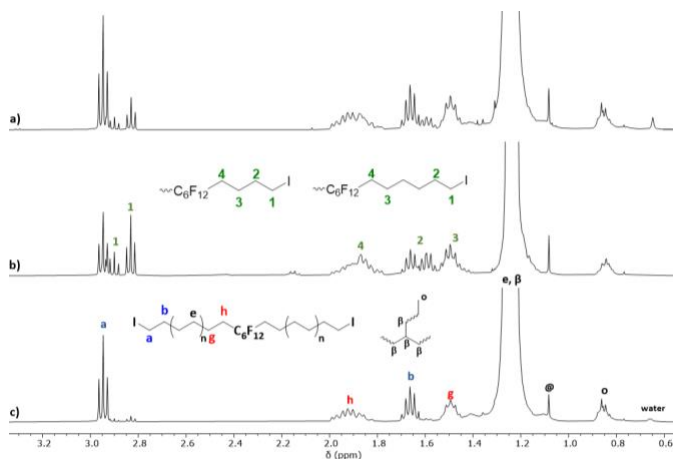


**Figure 4.**  $^1\text{H}$  NMR spectra (in  $\text{TCE}/\text{C}_6\text{D}_6$  at  $90^\circ\text{C}$ ) of PE synthesized at  $70^\circ\text{C}$ , 80 bar in the presence of CTA-1 after 45 min, a) before precipitation, b) of the residue obtained after evaporation of the filtrate and c) of the solid part obtained by precipitation. The end group  $-\text{CH}_3$  stems from intramolecular and intermolecular chain transfer inherent to ethylene radical polymerization. @ stems from the isobutyronitrile chain-ends of the PE chains initiated by AIBN. The water is in the NMR solvent.

$^{19}\text{F}$  NMR analyses were performed on the filtrate residue and solid products after precipitation of the PE (**Figure 5**). As expected in all cases, three signals are observed. The signals observed for the residue of the filtrate and for the precipitate are similar (**Figure 5b-c**) and differ from those of the starting CTA. This both confirms the formation of telechelic PE and that both iodines on the starting CTA-1 are activated after 45 min of polymerization.

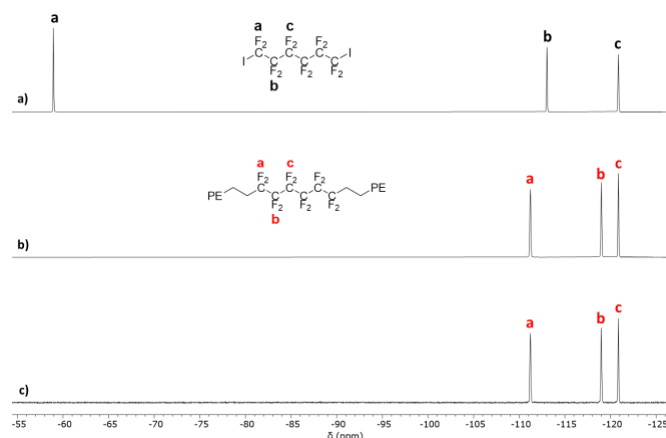


**Figure 5.**  $^{19}\text{F}$  NMR spectra (in  $\text{TCE}/\text{C}_6\text{D}_6$  at  $90^\circ\text{C}$ ) of a) CTA-1, and b) of the filtrate residue and c) the precipitated PE.

We tried to further characterize these structures by performing additional NMR analyses. From the  $^1\text{H}$ - $^1\text{H}$  COSY in **Figure S3** it is possible to correlate the triplets at 2.85 and 2.90 ppm with the multiplet at 1.60 ppm. The correlation spectrum has similarities with the spectra obtained when an iodine atom is connected to an ethylene unit. This observation, together with additional NMR analyses ( $^{13}\text{C}$  NMR and  $^1\text{H}$ - $^{13}\text{C}$  HSQC and HMBC - see **Figure S1** and **Figure S2** in supporting information) allowed us to assume that these signals could originate from non-symmetrical oligomers  $\text{I}-(\text{CH}_2-\text{CH}_2)_p\text{C}_6\text{F}_{12}(\text{CH}_2\text{CH}_2)_n\text{I}$  ( $n \neq p$ ,  $n+p \approx 7$ ) initiated by CTA-1. The asymmetry would result from the difference of reactivity of iodine atoms connected to primary carbon after the first additions of ethylene units reacted with CTA-1 and those still adjacent to  $-\text{CF}_2-$ . This is consistent with the disappearance of the triplet at 2.85 ppm after 6 h of reaction (**Figure 3d**), when all the iodine atoms had a chance to react many times to add ethylene units, and with the average molar mass of  $750\text{ g mol}^{-1}$  measured by NMR from **Figure 4b** after 45 min of reaction.

The presence of oligomers with different polymerization degree (up to 3 h of polymerization, **Figure 3c**) is somewhat surprising as this was not observed when polymerizations were mediated by CTA-2.<sup>35</sup> Nevertheless the broad SEC traces observed in the early stage of the polymerization in the latter case (**Figure 2** and

mentioned above) may find an explanation in similar phenomena. A hypothesis could be that when one iodine of CTA-1 has been involved in chain transfer reactions, chain transfer on the iodines on the resulting molecules may be different as a result of solubility, steric and/or electronic effects, leading to a mixture of asymmetric oligomers, the asymmetric nature fading away with the increase of the polymerization degree.

In order to confirm this hypothesis, we employed structurally similar molecular CTAs ( $C_6F_{13}CH_2-CH_2-I$  and  $C_5H_{10}-I$ , CTA-3 and CTA-4 respectively, **Scheme 1**) to mimic the early stage of the polymerization conducted with CTA-1. CTA-3 would mimic the reactivity of the molecule resulting from the addition of one ethylene unit and CTA-4 the reactivity of PE-I. A kinetic study was performed to compare the consumption of these different CTAs in the early stage of the polymerization. **Figure 6a** shows the CTA conversion and ethylene consumption *versus* polymerization time for the CTA-3 and the comparison with CTA-2 and CTA-4 mediated ITP of ethylene already studied in our group.<sup>35</sup> As already shown, CTA-2 is consumed almost instantly. However, the conversion rate of CTA-3 is slower than CTA-2, even if their structures are relatively close. Compared to CTA-2, CTA-3 possesses one ethylene unit between the  $C_6F_{13}$  group and the iodine. The fact that CTA-3 is converted faster than CTA-4, even if both CTAs present an iodo alkyl moiety  $-CH_2I$ , indicates the strong impact of the  $C_6F_{13}$  group on the reactivity and stabilization of the resulting  $C_6F_{13}CH_2CH_2\cdot$  radical.<sup>44</sup> This stabilizing effect will obviously be gradually reduced upon the addition of ethylene units to eventually induce a behaviour similar to CTA-4. These results confirm thus the simultaneous formation of asymmetric oligomers when using CTA-1 in the early stage of the polymerization.

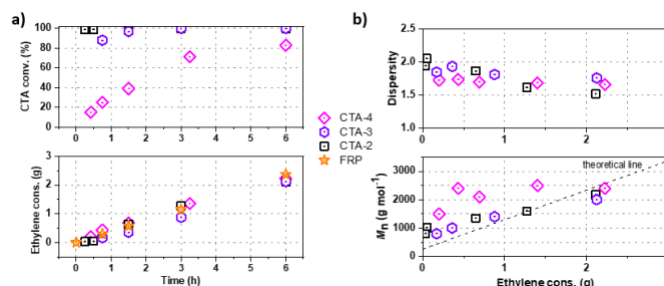


**Figure 6.** Polymerization conditions:  $T = 70\text{ }^{\circ}\text{C}$ ,  $P = 80\text{ bar}$ ,  $[\text{CTA}]:[\text{AIBN}] = 3:1$ . a) Ethylene consumption and CTA conversion *versus* polymerization time for ITP systems compared to radical ethylene polymerization performed without CTA, and b) corresponding molar mass evolutions (from HT-SEC). Molar masses are determined by a conventional PE calibration.

**Telechelic EVA copolymers.** Ethylene and VAc copolymerization by ITP (ITcOP) was successful in the presence of CTA-2.<sup>35</sup> This highly versatile system provides a simple tool for an easy access to a broad range of EVA containing from 0 to 85 mol% of VAc. Considering the excellent control observed for the ITP of ethylene mediated by CTA-1, we anticipated that ITcOP might be a powerful tool to produce telechelic P(E-co-VAc) from low to high contents of VAc. Thus, we subsequently studied the ITcOP of ethylene and VAc in the presence of CTA-1.

Copolymerizations were carried out with different quantities of VAc at different ethylene pressures at  $70\text{ }^{\circ}\text{C}$  in the presence of CTA-1 and AIBN ( $[\text{iodine}]:[\text{AIBN}] = 3:1$ ). Based on our previous works,<sup>35</sup> polymerization conditions were adjusted to target 25 mol%, 50 mol% and 65 mol% of VAc (**Table 1**, i.e. using 80 bar and 25 mL of VAc (runs 1-3), 60 bar and 37 mL of VAc (runs 4-7) and 40 bar and 37 mL of VAc (runs 8-11), respectively). For each VAc content, kinetic studies were performed to assess the polymerization control.

**Table 1.** ITcOPs of ethylene and VAc mediated by CTA-1.<sup>[a]</sup>

Run	Time (h)	Monomer cons. <sup>[b]</sup> (g)	$M_n(\text{theo})$ <sup>[c]</sup> ( $\text{g mol}^{-1}$ )	VAc content <sup>[d]</sup> (mol%)	$M_n(\text{NMR})$ <sup>[e]</sup> ( $\text{g mol}^{-1}$ )	$M_n(\text{SEC})$ <sup>[f]</sup> ( $\text{g mol}^{-1}$ )	$\mathcal{D}$ <sup>[f]</sup>	$T_m$ <sup>[g]</sup> ( $^{\circ}\text{C}$ )	$T_g$ <sup>[g]</sup> ( $^{\circ}\text{C}$ )
1 <sup>[h]</sup>	1.5	3.7	8600	27	9300	12900	1.5	-0.6	-29.6
2 <sup>[h]</sup>	3	7.8	17500	27	19000	17900	1.6	0.8	-30.5
3 <sup>[h]</sup>	6	14.5	31900	28	35100	33400	1.7	3.0	-30.2
4 <sup>[i]</sup>	0.75	5.6	12300	50	12800	15000	1.9	-	-6.9
5 <sup>[i]</sup>	1.5	11.0	24000	51	26100	25500	1.9	-	-8.5
6 <sup>[i]</sup>	3	20.3	44000	50	48200	37800	1.8	-	-8.2
7 <sup>[i]</sup>	6	26.0	58000	47	70700	38900	2.1	-	-7.8
8 <sup>[j]</sup>	0.75	6.3	14400	67	16800	18800	1.9	-	7.8
9 <sup>[j]</sup>	1.5	12.7	25800	64	28800	25850	1.8	-	9.0
10 <sup>[j]</sup>	3	23.4	52900	62	60900	34800	1.9	-	8.5
11 <sup>[j]</sup>	6	30.0	66100	61	72300	49100	2.1	-	5.0

[a] AIBN (0.3 mmol), CTA-1 (0.45 mmol) at  $70\text{ }^{\circ}\text{C}$  in DMC (total volume 50 mL). [b] Monomer consumption = (mass of dried product) - (mass of AIBN) - (mass of CTA). [c]  $M_n(\text{theo}) = (\text{monomer cons. [g]} / (\text{CTA [mol]})) + M_n(\text{CTA})$ . [d] Calculated by  $^1\text{H NMR}$  by comparing the  $\text{CH}_2$  signals of the ethylene units and the CH of the vinyl acetate units. [e] Calculated by comparing the  $^1\text{H NMR}$  signals of the EVA chain ( $\text{CH}_2$  of ethylene and CH of VAc) and the  $\text{CH}_2$  next to the iodo chain-end. [f] Determined by THF-SEC with a PS calibration. [g] Determined by DSC. [h] 80 bar, 25 mL of VAc. [i] 60 bar, 37 mL of VAc. [j] 40 bar, 37 mL of VAc.



The additional triplets seen by  $^1\text{H}$  NMR analyses in the early stage of the polymerization (45 min) at around 2.85 ppm in the case of ITP of ethylene mediated by CTA-1 (**Figure 3**) are no longer visible in the EVAs obtained after 45 min of polymerization. This observation however does not tell that they cannot form earlier as a result of a faster propagation in the presence of VAc.  $^{19}\text{F}$  NMR analyses were carried out on the final copolymers (**Figure S4**). The corresponding spectra were similar to those obtained during the ethylene homopolymerization shown in **Figure 5c**, indicating that both iodines on CTA-1 were activated.  $^1\text{H}$  NMR analyses confirm indeed the expected iodo-end-capped EVA species by showing the characteristic signal assigned to  $-\text{CH}_2\text{I}$  at around 3 ppm (spectra were measured in  $\text{CDCl}_3$  and this signal is at 3.15 ppm, the same signal being at 2.95 ppm when the analysis is performed in  $\text{TCE}/\text{C}_6\text{D}_6$ ) (**Figure 7**). The shape of this signal evolves from a clean triplet to a broad signal with increasing the VAc content. Similar behaviors were already seen when synthesizing EVAs at different VAc contents by RAFT<sup>33</sup> and ITP.<sup>35</sup> Indeed, a terminal ethylene-iodine unit is less readily reactivated than a terminal VAc-iodine unit. This results in iodine chain-ends connected to an ethylene unit rather than to a VAc unit. However, when increasing the VAc contents in the chains, the increasing probability of having a penultimate VAc units affects the chemical shift of the  $-\text{CH}_2\text{I}$  protons of the terminal ethylene unit leading to the broadening observed in **Figure 7**. The same phenomenon could explain the presence of signals of small intensity present between -109 and -112 ppm in **Figure S4**. Eventually, the results showed a good consistency between the expected molar masses and the ones measured by NMR using these chain-end signals (**Table 1**), attesting that ITCoP of ethylene and VAc mediated by CTA-1 led to a high chain-end fidelity.

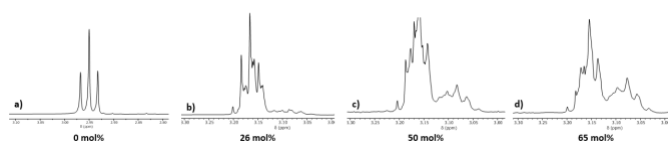


**Figure 7.**  $^1\text{H}$  NMR resonances in a)  $\text{TCE}/\text{C}_6\text{D}_6$  at 90 °C and b-d)  $\text{CDCl}_3$  at 25 °C, between 2.80 and 3.40 ppm stemming from the  $\text{CH}_2$  protons adjacent to the iodine atom at different VAc content after 6 h of polymerization.

This is further evidenced for all three systems in **Figure 8** as the corresponding unimodal molar mass distributions are nicely

shifted toward higher molar masses with polymerization times. It should be noted that for the  $\text{P}(\text{E-co-VAc})$  copolymers, the  $M_n$  and  $\mathcal{D}$  values obtained from SEC analyses should be taken with caution. Different ethylene contents might lead to different elution behavior during the SEC analysis, which might not be adequately reflected by the use of PS standards for the calibration. This is particularly true for targeted molar masses higher than  $40000 \text{ g mol}^{-1}$  (runs 6, 7, 10, and 11 in **Table 1**). We thus considered the molar mass data obtained from NMR spectroscopy for a quantitative comparison of the  $M_n$  values of the copolymers.

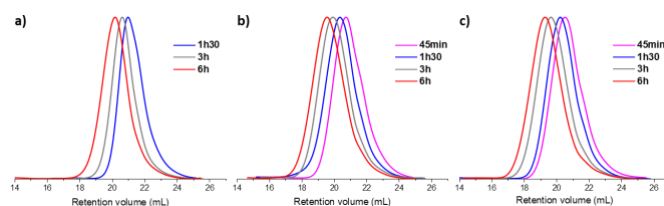


**Figure 8.** Molar mass distributions of  $\text{P}(\text{E-co-VAc})$  obtained during the ITCoP of ethylene and VAc mediated by CTA-1 with a VAc content of ca. a) 27 mol% (runs 1-3), b) 50 mol% (runs 4-7), and c) 64 mol% (runs 8-11).

Eventually, and as expected, the telechelic copolymers exhibit melting and glass transition temperatures comparable with those already obtained for their monofunctional analogue using ITP, with a  $T_g$  that can be tuned by the VAc content (**Table 1**).<sup>35</sup>

**Triblock copolymers based on ethylene and vinyl acetate.** The above demonstrated easy access to  $\alpha-\omega$ -iodo telechelic PE or EVA gives an easy access to difunctional ITP macromolecular chain transfer agent (macroCTA) and thus to potential ABA triblock architectures. We thus next investigated the synthesis of triblock copolymers based on ethylene and VAc.

Indeed, I-EVA-I telechelic copolymers were further used as difunctional macroCTA for the polymerization of ethylene to reach PE-*b*-EVA-*b*-PE triblock copolymers. Chain extensions were carried out for 2 h at 80 bar and 80 °C in the presence of the telechelic EVA macroCTA. For clarity sake, macroCTA containing  $x \text{ mol}\%$  of VAc is referred to as  $\text{EVA}_{x\%}$  in the following.  $\text{EVA}_{27\%}$  and  $\text{EVA}_{64\%}$  (respectively runs 1 and 9, in **Table 1** and **Table 2**) were used to target two different ABA triblock: PE-*b*- $\text{EVA}_{27\%}$ -*b*-PE and PE-*b*- $\text{EVA}_{64\%}$ -*b*-PE (runs 12 and 13 in **Table 2**, respectively). Having respectively  $T_g$  of -29.6 °C and 9.0 °C,  $\text{EVA}_{27\%}$  and  $\text{EVA}_{64\%}$  were chosen as two representative EVAs with  $T_g$ s below and close to room temperature.

**Table 2.** Chain extensions of telechelic EVA macroCTAs.<sup>[a]</sup>

Run	Name	Monomer cons. <sup>[b]</sup> (g)	$M_n$ (theo.) <sup>[c]</sup> (g mol <sup>-1</sup> )	VAc content <sup>[d]</sup> (mol%)	$M_n$ (NMR) <sup>[e]</sup> (g mol <sup>-1</sup> )	$M_n$ (SEC) <sup>[f]</sup> (g mol <sup>-1</sup> )	$\bar{D}$ <sup>[f]</sup>	$T_m$ <sup>[g]</sup> (°C)	$X$ <sup>[g]</sup> (%)	$T_g$ <sup>[g]</sup> (°C)
1	EVA <sub>27%</sub>	3.7	8600	27	9300	12900	1.5	-0.6	0.4	-29.6
9	EVA <sub>64%</sub>	12.7	25800	64	28800	25850	1.8	-	-	9.0
12 <sup>[h]</sup>	PE- <i>b</i> -EVA <sub>27%</sub> - <i>b</i> -PE	1.4	15500	0-27-0 <sup>[i]</sup>	18700	/	/	113.2	19.8	-29.4
13 <sup>[j]</sup>	PE- <i>b</i> -EVA <sub>64%</sub> - <i>b</i> -PE	1.5	32000	0-64-0 <sup>[j]</sup>	35300	/	/	112.2	9.5	5.1

[a] AIBN (0.15 mmol), macroCTA (0.23 mmol) at 80 °C and 80 bar in DMC (50 mL) for 2 h. [b] Monomer consumption = (mass of dried product) - (mass of AIBN) - (mass of macroCTA). [c]  $M_n$ (theo.) = (monomer cons. [g]) / (macroCTA [mol]) +  $M_n$ (macroCTA). [d] Calculated by <sup>1</sup>H NMR by comparing the CH<sub>2</sub> signals of the ethylene units and the CH of the vinyl acetate units. [e] Calculated by comparing the <sup>1</sup>H NMR signals of the EVA chain (CH<sub>2</sub> of ethylene and CH of VAc) and the CH<sub>2</sub> next to the iodo chain-end. [f] Determined by THF-SEC with a PS calibration. [g] Determined by DSC. [h] Chain extension of EVA from run 1. [i] Chain extension of EVA from run 9. [j] EVA content of the 2<sup>nd</sup> block-1<sup>st</sup> block-2<sup>nd</sup> block.

The corresponding SEC traces are presented in **Figure 9**. A clear shift of the molar mass distributions towards lower elution volumes is observed in both cases, indicating successful chain extension of the starting EVAs.

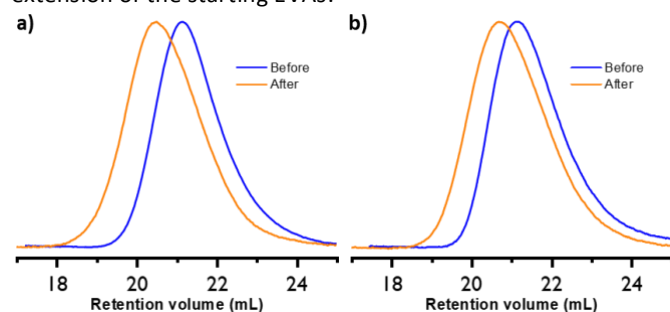


**Figure 9.** Evolution of molar mass distributions after the chain extension in the presence of ethylene of a) EVA<sub>27%</sub> (runs 1 and 12 in **Table 2**) and b) EVA<sub>64%</sub> (runs 9 and 13 in **Table 2**)

The corresponding <sup>1</sup>H NMR spectra for the chain extension of EVA<sub>64%</sub>, recorded in TCE/C<sub>6</sub>D<sub>6</sub>, are presented in **Figure 10**. Considering the comment made on the shape of the triplet at 2.95 ppm observed when analyzing EVA by <sup>1</sup>H NMR, it is quick and easy to identify if chain extension with ethylene cleanly takes place. Indeed, the distorted signal at ca. 2.95 ppm stemming from the terminal -CH<sub>2</sub>I in EVA<sub>64%</sub> (**Figure 10a**) transforms into a clean triplet in **Figure 10b** after chain extension with ethylene. This is consistent with the earlier explained effect that a penultimate VAc unit affects the chemical shift of the -CH<sub>2</sub>I protons and further confirms the installation of a PE segment on EVA<sub>64%</sub> and thus the successful formation of PE-*b*-EVA<sub>64%</sub>-*b*-PE. Furthermore, a good match between experimental and expected  $M_n$  values was observed:  $M_n$ (NMR) = 18700 g mol<sup>-1</sup> vs  $M_n$ (theo.) = 15500 g mol<sup>-1</sup> and  $M_n$ (NMR) = 35300 g mol<sup>-1</sup> vs  $M_n$ (theo.) = 32000 g mol<sup>-1</sup> for PE-*b*-EVA<sub>27%</sub>-*b*-PE and PE-*b*-EVA<sub>64%</sub>-*b*-PE, respectively. Telechelic EVAs thus prove to be efficient macroCTAs to synthesize PE-*b*-EVA-*b*-PE triblock copolymers.

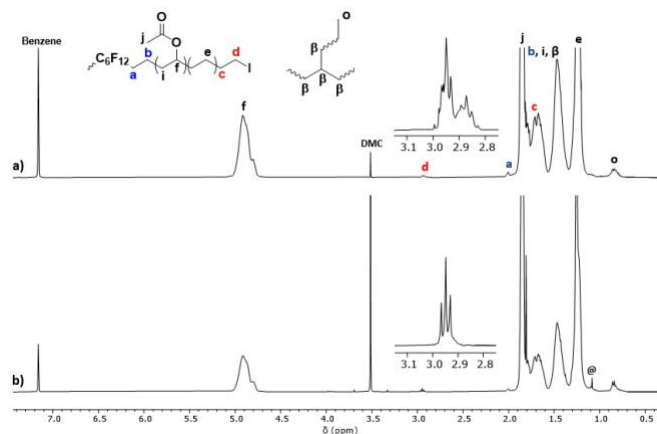


**Figure 10.** <sup>1</sup>H NMR spectra (in TCE/C<sub>6</sub>D<sub>6</sub> at 90 °C) of a) starting EVA<sub>64%</sub>, and b) PE-*b*-EVA<sub>64%</sub>-*b*-PE after chain extension (**Table 2**, runs 9 and 13).

In terms of thermal properties, these triblock copolymers should display both a melting temperature ( $T_m$ ) originating from the hard PE blocks and a glass transition temperature ( $T_g$ ) originating from the soft central EVA block.  $T_m$  is similar in both triblock copolymers (around 113 °C, **Table 2**), close to the  $T_m$  of PE made by ITP under the same conditions<sup>35</sup>. Depending on the macroCTA,  $T_g$  were measured at -29.4 °C for PE-*b*-EVA<sub>27%</sub>-*b*-PE and at 5.1 °C for PE-*b*-EVA<sub>64%</sub>-*b*-PE. These  $T_g$ s are, as expected, very close to those of the starting macroCTA (-29.6 and 9.0 °C for EVA<sub>27%</sub> and EVA<sub>64%</sub>, respectively).

## Conclusions

In conclusion, a difunctional iodide CTA, I-C<sub>6</sub>F<sub>12</sub>-I, as established as a powerful CTA to synthesize well-defined telechelic PEs by ITP. The very first ethylene additions resulted in the formation of iodo compounds with various chain transfer activities. This was revealed by <sup>1</sup>H NMR analyses that showed the formation of the corresponding species in the early stage of the polymerization. This however did not impact the control of the polymerization which resulted in well-defined telechelic I-PE-I homopolymers. Strong of these results, telechelic I-EVA-I copolymers of the same quality were also synthesized by ITPcoP of ethylene and vinyl acetate. They were further used as macroCTA in chain extension experiments in the presence of ethylene to lead to hard-soft-hard PE-*b*-EVA-*b*-PE triblock copolymers with different content of VAc in the central block.



The present study shows the versatility that ITcoP can offer to access a wide range of materials based on monomers of industrial interest such as ethylene and vinyl acetate, potentially including thermoplastic elastomers.

## Acknowledgements

F.B. acknowledges the French Ministère de l'Enseignement Supérieur de la Recherche et de l'Innovation (MESRI) for funding.

## Conflicts of interest

There are no conflicts to declare.

## Notes and references

1. A. J. Peacock, *Handbook of polyethylene: structures, properties, and applications*, Marcel Dekker, New York, 2000.
2. T. C. Chung, *Prog. Polym. Sci.*, 2002, **27**, 39-85.
3. R. Godoy Lopez, F. D'Agosto and C. Boisson, *Prog. Polym. Sci.*, 2007, **32**, 419-454.
4. A. Nakamura, S. Ito and K. Nozaki, *Chem. Rev.*, 2009, **109**, 5215-5244.
5. N. M. G. Franssen, J. N. H. Reek and B. d. Bruin, *Chem. Soc. Rev.*, 2013, **42**, 5809-5832.
6. A. Keyes, H. E. Basbug Alhan, E. Ordonez, U. Ha, D. B. Beezer, H. Dau, Y.-S. Liu, E. Tsogetgerel, G. R. Jones and E. Harth, *Angew. Chem. Int. Ind.*, 2019, **58**, 12370-12391.
7. P. D. Goring, C. Morton and P. Scott, *Dalton Trans.*, 2019, **48**, 3521-3530.
8. M. A. Tasdelen, M. U. Kahveci and Y. Yagci, *Prog. Polym. Sci.*, 2011, **36**, 455-567.
9. T. Yan and D. Guironnet, *Polym. Chem.*, 2021, **12**, 5126-5138.
10. M. L. Poutsma, *Macromolecules*, 2003, **36**, 8931-8957.
11. T. Shiono, N. Naga and K. Soga, *Makromol. Chem. Rapid Commun.*, 1991, **12**, 387-392.
12. T. Shiono, N. Naga and K. Soga, *Makromol. Chem. Rapid Commun.*, 1993, **14**, 323-327.
13. F. Lucas, F. Peruch, S. Carlotti, A. Deffieux, A. Leblanc and C. Boisson, *Polymer*, 2008, **49**, 4935-4941.
14. K. Sill and T. Emrick, 2005, **43**, 5429-5439.
15. L. M. Pitet, M. A. Amendt and M. A. Hillmyer, *J. Am. Chem. Soc.*, 2010, **132**, 8230-8231.
16. L. M. Pitet and M. A. Hillmyer, *Macromolecules*, 2011, **44**, 2378-2381.
17. L. Annunziata, S. Fouquay, G. Michaud, F. Simon, S. M. Guillaume and J.-F. Carpentier, *Polym. Chem.*, 2013, **4**, 1313-1316.
18. H. Martinez and M. A. Hillmyer, *Macromolecules*, 2014, **47**, 479-485.
19. A. C. Gottfried and M. Brookhart, *Macromolecules*, 2003, **36**, 3085-3100.
20. H. Makio and T. Fujita, *Macromol. Rapid Commun.*, 2007, **28**, 698-703.
21. S. Park, T. Okada, D. Takeuchi and K. Osakada, *Chem. Eur. J.*, 2010, **16**, 8662-8678.
22. Z. Jian, L. Falivene, G. Boffa, S. O. Sánchez, L. Caporaso, A. Grassi and S. Mecking, *Angew. Chem. Int. Ind.*, 2016, **55**, 14378-14383.
23. I. German, W. Kelhifi, S. Norsic, C. Boisson and F. D'Agosto, *Angew. Chem. Int. Ind.*, 2013, **52**, 3438-3441.
24. H. Makio, T. Ochiai, J.-i. Mohri, K. Takeda, T. Shimazaki, Y. Usui, S. Matsuura and T. Fujita, *J. Am. Chem. Soc.*, 2013, **135**, 8177-8180.
25. M. G. Hyatt and D. Guironnet, *ACS Catal.*, 2017, **7**, 5717-5720.
26. W. Nzahou Ottou, S. Norsic, I. Belaid, C. Boisson and F. D'Agosto, *Macromolecules*, 2017, **50**, 8372-8377.
27. W. N. Ottou, S. Norsic, F. D'Agosto and C. Boisson, *Macromol. Rapid Commun.*, 2018, **39**, 1800154.
28. S. Yamago and Y. Lu, in *Free Radicals: Fundamentals and Applications in Organic Synthesis 2*, Georg Thieme Verlag KG, Stuttgart, 2021, vol. 2020/5.
29. S. Borkar and A. Sen, 2005, **43**, 3728-3736.
30. S. Liu, B. Gu, H. A. Rowlands and A. Sen, *Macromolecules*, 2004, **37**, 7924-7929.
31. C. Dommanget, F. D'Agosto and V. Monteil, *Angew. Chem. Int. Ind.*, 2014, **53**, 6683-6686.
32. A. Wolpers, C. Bergerbit, B. Ebeling, F. D'Agosto and V. Monteil, *Angew. Chem. Int. Ind.*, 2019, **58**, 14295-14302.
33. A. Wolpers, F. Baffie, V. Monteil and F. D'Agosto, *Macromol. Rapid Commun.*, 2021, **42**, 2100270.
34. Y. Nakamura, B. Ebeling, A. Wolpers, V. Monteil, F. D'Agosto and S. Yamago, *Angew. Chem. Int. Ind.*, 2018, **57**, 305-309.
35. A. Wolpers, F. Baffie, L. Verrieux, L. Perrin, V. Monteil and F. D'Agosto, *Angew. Chem. Int. Ind.*, 2020, **59**, 19304-19310.
36. A. Kermagoret, A. Debuigne, C. Jérôme and C. Detrembleur, *Nat. Chem.*, 2014, **6**, 179-187.
37. J. Demarteau, J. De Winter, C. Detrembleur and A. Debuigne, *Polym. Chem.*, 2018, **9**, 273-278.
38. J. Demarteau, P. B. V. Scholten, A. Kermagoret, J. De Winter, M. A. R. Meier, V. Monteil, A. Debuigne and C. Detrembleur, *Macromolecules*, 2019, **52**, 9053-9063.
39. E. Pouget, J. Tonnar, C. Eloy, P. Lacroix-Desmazes and B. Boutevin, *Macromolecules*, 2006, **39**, 6009-6016.
40. A. D. Asandei, O. I. Adebolu and C. P. Simpson, *J. Am. Chem. Soc.*, 2012, **134**, 6080-6083.
41. L. Lei, M. Tanishima, A. Goto, H. Kaji, Y. Yamaguchi, H. Komatsu, T. Jitsukawa and M. Miyamoto, *Macromolecules*, 2014, **47**, 6610-6618.
42. M. Tanishima, A. Goto, L. Lei, A. Ohtsuki, H. Kaji, A. Nomura, Y. Tsujii, Y. Yamaguchi, H. Komatsu and M. Miyamoto, *Polymers*, 2014, **6**, 311-326.
43. P. Černoch, Z. Černochová, S. Petrova, D. Kaňková, J.-S. Kim, V. Vasu and A. D. Asandei, *RSC Adv.*, 2016, **6**, 55374-55381.
44. R. Poli, S. M. W. Rahaman, V. Admiral and B. Ameduri, *J. Organomet. Chem.*, 2018, **864**, 12-18.

